ELSEVIER

Biophysical Chemistry 59 (1996) 299–314

Biophysical Chemistry

Investigation of electrostatic interactions in two-stranded coiled-coils through residue shuffling [1]

Yihua Yu [a], Oscar D. Monera [b], Robert S. Hodges [b], Peter L. Privalov [a,*]

[a] *Department of Biophysics and Department of Biology, The Johns Hopkins University, 3400 N. Charles St., Baltimore, MD 21218, USA*
[b] *Department of Biochemistry and the Protein Engineering Network of Centres of Excellence, University of Alberta, Edmonton, Alberta T6G 2H7, Canada*

Abstract

The effects of electrostatic interactions on the stability of coiled-coils were investigated using the strategy of shuffling the sequence without changing the overall content of amino acid residues in the peptides. Shuffling the sequence provides peptides with thermodynamically similar unfolded states. Therefore, the unfolded state can be used as a universal reference state in comparing the thermodynamic properties of the folded coiled-coil structure of the peptides, while varying the configuration of ionized groups, that is, changing the types and number of potential electrostatic interactions. The relative stabilities of these states were determined by monitoring the temperature-induced folding/unfolding of the peptides in solutions with different pH and ionic strength by circular dichroism spectroscopy and scanning microcalorimetry. It was found that, in solutions with low ionic strength, ionic pairs contribute significantly to the stability of the coiled-coil conformation. The stability increases with an increase in the number of ionized groups in the peptide upon changing pH from acidic to neutral. In contrast, in the solutions with high ionic strength, the coiled-coil becomes less stable at neutral pH than at acidic pH. Most surprisingly, the increase in Gibbs energy of stabilization of the coiled-coil state with increasing pH at low ionic strength proceeds with a decrease in the enthalpy and entropy of unfolding. This observation can be explained only by hydration of ionized groups upon unfolding of coiled-coils which is associated with significant negative enthalpy and entropy effects.

Keywords: Coiled-coils; Circular dichroism; Electrostatic interactions; Thermodynamics; Calorimetry; Sequence variation

1. Introduction

Protein folding is one of the central problems for understanding life at the molecular level. It is clear that protein folding is a thermodynamically driven process [1]. However, the molecular forces determining this process are still obscure [2]. A useful experimental approach to this problem is to study the unfolding/refolding of native proteins and various de novo designed synthetic polypeptide models. The latter became especially attractive with the development of efficient methods of polypeptide synthesis. The synthetic peptide minimalistic approach allows the design of the desired features of protein structure and to create simplified models which are easier for

* Corresponding author.

[1] We dedicate this paper to the memory of Professor Bill Harrington. Professor Harrington believed that the melting of coiled-coils played a significant role in muscle contraction which greatly enhanced the interest for understanding the energetics of their structure.

SSDI 0301-4622(95)00131-X

both experimental and theoretical analysis, and open prospects for the design of artificial proteins.

One of the most attractive models for studying protein folding is the two-stranded α-helical coiled-coil [3–5]. The current interest in coiled-coils is due not only to the great biological significance of this type of structure which is basic for many proteins [6–9], and particularly for muscle proteins, in which their unfolding/refolding might have a principal importance for transferring the chemical energy into mechanical work [10,11]. Two-stranded coiled-coils are the simplest among the stable, highly cooperative protein models which have yet been synthesized [12–20]. The simplicity and regularity in their structural organization opens a unique possibility in using sequence variation for investigating the contribution of various factors stabilizing their structure, namely the shuffling of amino acid residues without changing their content in the peptides studied.

The main forces stabilizing the α-helical coiled-coil conformation are assumed to be hydrophobic interactions between non-polar groups on the contact faces of two intertwined α-helices [3,21]. There are also charged groups in the coiled-coil which are arranged in a quite specific configuration, suggesting the importance of electrostatic interactions in the stabilization of their folded state [22]. However, the role played by electrostatics in stabilizing coiled-coils is still puzzling: it has been widely observed that coiled-coils are more stable at acidic pH, where ionic pairs are absent, than at neutral pH, where ionic pairs are present [6,7,13–17,23]. Most recently, there is report that an ion pair in a leucine zipper coiled-coil is destabilizing [24]. To investigate the role of electrostatic interactions in stabilization of coiled-coils we designed a set of peptides which differ only in configuration of ionized groups in the coiled-coil conformation, that is, in the content of electrostatic interactions.

2. Description of models and strategy of sequence variation

Our strategy for generating peptides differing in electrostatic interactions in the coiled-coil state consisted of shuffling residues already in the sequence rather than making substitutions that will introduce new residues into the polypeptide chain. The shuffling of residues is done in such a way as to preserve as much as possible both the sequential context and tertiary contacts of the permutation sites. Shuffling of residues should not induce significant change in thermodynamics of the unfolded state because the sequential context is very similar at the permutation sites. Therefore, residual structure in the unfolded state will be virtually the same for different peptides (Fig. 1). As a result, the unfolded state can be used as a universal reference state in comparing the thermodynamic properties of the coiled-coil state of all the peptides generated by residue shuffling. The difference between any two peptides will arise from a single type of interaction only in the folded form. Using the residue shuffling strategy, we generated the sequences of coiled-coil peptides listed in Table 1. The configuration of ionizable residues in these peptides and putative electrostatic interactions between them are presented in Fig. 2 and Table 2.

As shown for the central heptad in Fig. 2, three chargeable residues, two lysines and one glutamate, are incorporated into each heptad of the coiled-coils to form four pairs of potential electrostatic interactions with different configurations. Of the four pairs of interactions, two $(i, i' + 5)$ are interchain and two $(i, i + 3)$ are intrachain. In addition, each chain also contains four potential $(i, i + 4)$ intrachain electrostatic interactions for a total of eight pairs in the two stranded coiled-coil, as shown in Fig. 3. However for simplicity, the peptide nomenclature is based on the number of $(i, i' + 5)$ interchain and $(i, i + 3)$ intrachain electrostatic interactions which are identical in each heptad. For example, when all three ionizable residues are charged, $(2A)^{er}(2A)^{ra}$ represents the peptide with two interchain (er) and two intrachain (ra) electrostatic attractions (A). Similarly, $(1A1R)^{er}(2A)^{ra}$ represents the peptide with one interchain attraction (A) and one interchain repulsion (R) and two intrachain attractions (A). The same system is used for the remaining peptides which are shown in Table 2 with their corresponding total number of potential electrostatic interactions at pH 2.0 (when Glu is not ionized) and 6.5 (when Glu is ionized). These different electrostatic configurations are obtained by merely permutating the positions of the chargeable residues in each helix. Therefore, the composition and charge density are invariant

throughout the set of peptides. A more subtle quantity, the intrinsic helix propensity, is also invariant. Due to its uncertainty [25–29], exact cancellation is the only way to get rid of interference from this factor. Features built into the sequence to make the environment of the permutation sites as similar as possible include: (a) the hydrophobic core is kept invariant; (b) two identical serine residues are taken to occupy the boundary between the two charge strips in each helix (see Fig. 2); (c) interchain attractions are always between K(g) and E(e'), but not the other way around, that is, E(g) and K(e').

In constructing the peptides other measures were also taken to:

(1) Maximize solubility while minimizing potential chemical modification of residues at high temperature [30,31]. This is the reason that two serines were selected as the identical pair mentioned above.

(2) Avoid formation of four-stranded coiled-coils. This was achieved by putting an alanine at position 17 in each peptide chain [32].

(3) Cross-link two polypeptides forming the coiled-coil. This was done by placing cysteine at the N-terminal ends of the polypeptide and connecting them with a disulfide bond. This is necessary to keep two chains in register and to make the unfolding a unimolecular process. It also prevents heterodimer dissociation and formation of a mixture of homo- and heterodimers.

(4) Exclude influence of N- and C-terminal charges on the electrostatic interactions in coiled-coils. This was done by blocking the termini by neutral groups.

(5) Measure concentration of polypeptides spectrophotometrically. For this reason a tyrosine is placed at the N-terminal end of each polypeptide.

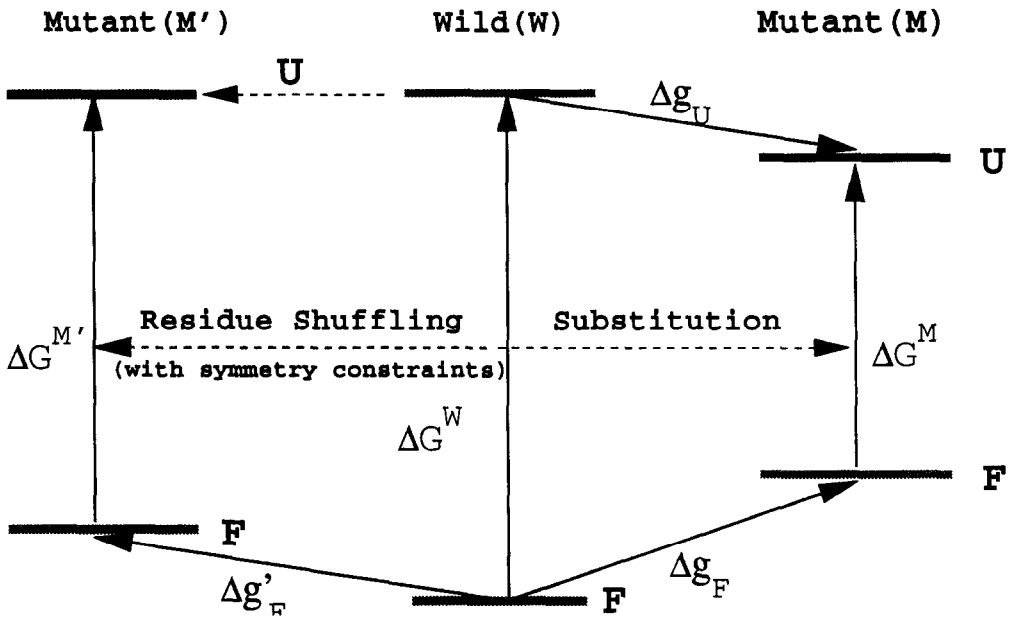

Fig. 1. Comparison of energy states between residue shuffling and substitution schemes. F means folded and U means unfolded states. Δg is the free energy difference between the mutant and the wild protein at the same state (folded or unfolded). ΔG is the free energy difference between the unfolded and the folded forms of the same protein. Possible interactions that contribute to each quantity are given. Δg_F: hydrophobicity, helix propensity, charge density, hydrogen bonding, salt bridges, packing effect, etc. Δg_U: residual structure, side chain entropy and hydration, charge density, etc. $\Delta g'_F$: difference in the folded form due to a single type of interaction (e.g., electrostatics, packing) between a specific pairs of residues.

3. Materials and methods

3.1. Peptide synthesis and purification

The peptides were synthesized by standard solid-phase methodology and purified by reversed-phase high-performance liquid chromatography (HPLC). The disulfide bond was formed by air oxidation in 100 mM NH_4HCO_3 at pH 8. For peptide combinations that do not readily form heterodimers, air oxidation was conducted in 100 mM NH_4HCO_3, pH 8, containing 6 M guanidinium hydrochloride. In each case, the heterodimer was separated from the two concomitant homodimers by reversed-phase HPLC. Because all disulfide-bridged products have identical amino acid composition and molecular weight as well as charge density, the homodimers were identified by coinjection with two independently prepared homodimers and the third product peak was taken as the heterodimer. The authenticity of disulfide bridge formation was verified by mass spectrometry. Details of the synthesis and purification procedures were similar to those described previously [13,17,32,33]. The two-strandedness of the peptides was verified by size-exclusion chromatography. All peptides are two-stranded monomers, except for $(2R)^{er}(2R)^{ra}$, which showed a broad peak that suggests some aggregation.

Table 1
Sequences of coiled-coil peptides

peptide[c]	sequence[a] (g a b c d e f g a b c d a d a d a d)[b]	chain type
$(2A)^{er}(2A)^{ra}$ homostranded	*Ac*-YKCKSLESKVKSLESKAKSLESKVKSLESKVKSLES-*am* | *Ac*-YKCKSLESKVKSLESKAKSLESKVKSLESKVKSLES-*am*	1 1
$(1A1R)^{er}(2A)^{ra}$ heterostranded	*Ac*-YKCKSLESKVKSLESKAKSLESKVKSLESKVKSLES-*am* | *Ac*-YKCESLKSKVESLKSKAESLKSKVESLKSKVESLKS-*am*	1 2
$(2A)^{er}(1A1R)^{ra}$ heterostranded	*Ac*-YKCKSLESKVKSLESKAKSLESKVKSLESKVKSLES-*am* | *Ac*-YKCSKLESKVSKLESKASKLESKVSKLESKVSKLES-*am*	1 3
$(2R)^{er}(2A)^{ra}$ homostranded	*Ac*-YKCESLKSKVESLKSKAESLKSKVESLKSKVESLKS-*am* | *Ac*-YKCESLKSKVESLKSKAESLKSKVESLKSKVESLKS-*am*	2 2
$(2A)^{er}(2R)^{ra}$ homostranded	*Ac*-YKCSKLESKVSKLESKASKLESKVSKLESKVSKLES-*am* | *Ac*-YKCSKLESKVSKLESKASKLESKVSKLESKVSKLES-*am*	3 3
$(2R)^{er}(2R)^{ra}$ heterostranded	*Ac*-YECKSLKSEVKSLKSEAKSLKSEVKSLKSEVKSLKS-*am* | *Ac*-YKCSKLESKVSKLESKASKLESKVSKLESKVSKLES-*am*	4 3

[a] Residues involved in shuffling are underlined. All these disulfide-bridged two-stranded coiled-coils have the same amino acid composition but different sequences.

[b] Letters in the parentheses indicate positions in each heptad.

[c] Superscripts er and ra stand for inter- and intra-chain electrostatic interactions, respectively. A and R denote electrostatic attractions and repulsions, respectively, as shown in Fig. 2.

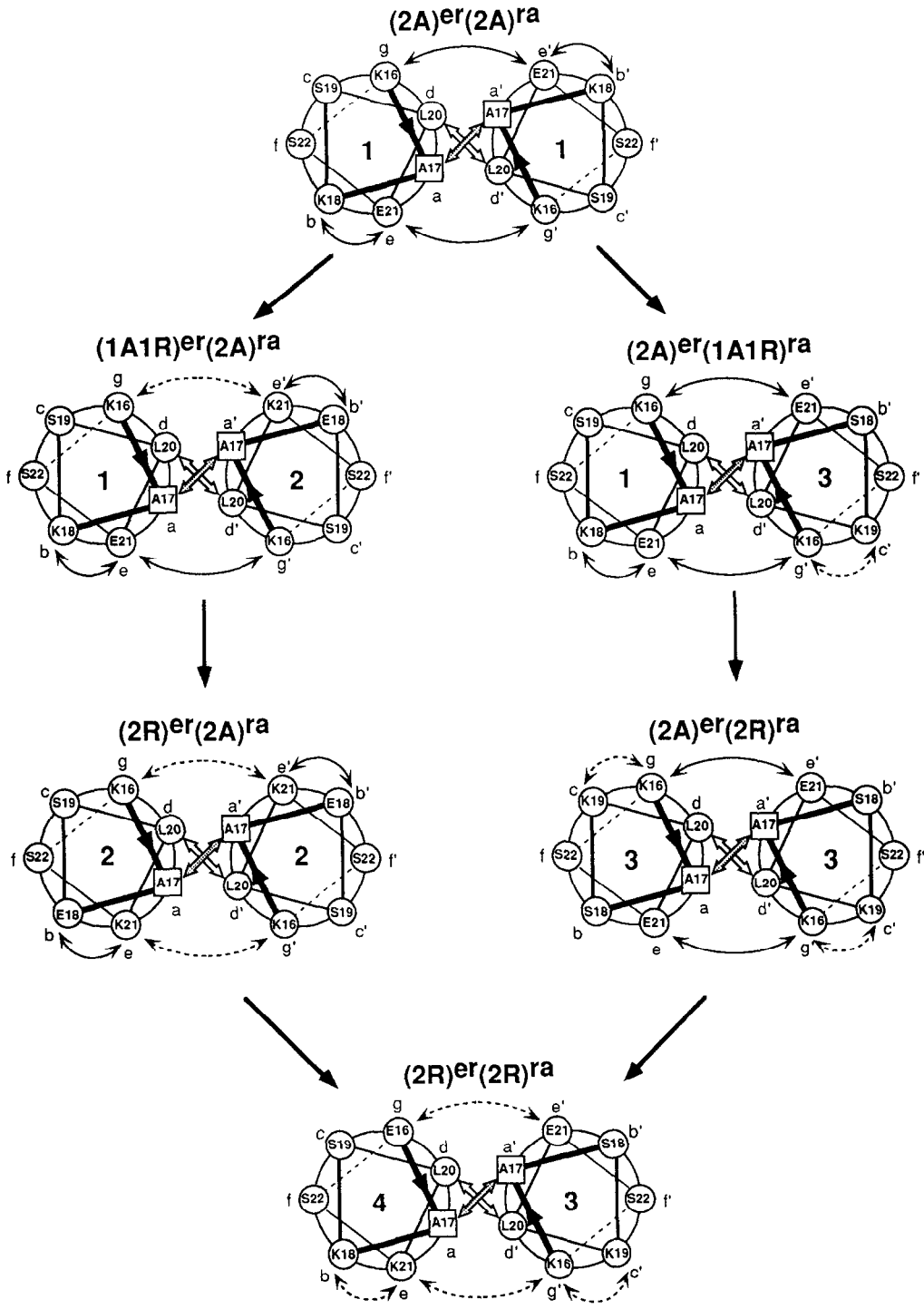

Fig. 2. Helical-wheel representation of the peptide set generated by residue shuffling. Only the middle heptad of each peptide is shown here. Letters a, b, c, d, e, f, g denote the positions of each residue in the heptad repeat. Electrostatic attractions are represented by solid arrows while electrostatic repulsions are represented by dashed arrows.

3.2. Solution preparation

Buffers used for circular dichroism (CD) and calorimetric measurements are: at pH 2.0, phosphoric acid; at pH 2.5–3.5, glycine–HCl; at pH 4.0–5.5, 10 mM sodium acetate–NaOH, 1.0 mM EDTA; at pH 6.0–7.5, 10 mM sodium phosphate, 1.0 mM EDTA and at pH 8.0–10.0, 10 mM boric acid–NaOH, 1.0 mM EDTA. For CD measurement, the peptide stock solution was dialyzed against deionized water, then diluted by appropriate buffer to the desired pH. For calorimetric measurement, each peptide was dialyzed against buffer of desired pH directly. Concentration was determined by measuring UV absorption at 275 nm in 5–6 M guanidinium hydrochloride of pH 6.5. The extinction coefficient is 0.375 a.u. mg^{-1} ml at 275 nm, calculated from the amino acid composition according to Gill and Von Hippel [34]. Light scattering effect was corrected for according to Winder and Gent [35].

3.3. Circular dichroism spectroscopy

Ellipticity was measured using a Jasco 710 spectropolarimeter, calibrated with *d*-10-camphorsulfonate. Structural changes induced by heating were monitored as the change in molar ellipticity at 222 nm with a heating rate of 0.5°C min^{-1}.

3.4. Differential scanning calorimetry

Calorimetric measurements were carried out on scanning microcalorimeters developed at the Biocalorimetry Center at the Johns Hopkins University, following standard procedure for sample preparation and data retrieval [36]. In all measurements, the heating rate was 1°C min^{-1}. The partial molar heat capacity of a fully extended peptide is calculated from its amino acid composition according to Privalov and Makhatadze [37]. Partial specific volume of the peptides was calculated from amino acid composition according to Makhatadze et al. [38] with a value of 0.751 ml mg^{-1}.

Reversibility of heat denaturation is checked both optically, by the ellipticity, and calorimetrically, by the heat capacity and enthalpy. At acidic pH, the reversibility is about 100% upon heating up to 100°C. At neutral pH, reversibility is 90% upon heating to 85°C, and decreases upon heating to higher temperatures.

Table 2
Overall electrostatic configurations and molar ellipticities of coiled-coils at pH 2.0 and 6.5 [a]

Peptide [b]	Type	pH 2.0		pH 6.5	
		Electrostatic interactions [c]	$[\theta_{222}]$ [d] (deg cm^2 $dmol^{-1}$)	Electrostatic interactions [c]	$[\theta_{222}]$ [d] (deg cm^2 $dmol^{-1}$)
$(2A)^{er}(2A)^{ra}$	intrachain	0 [e]	−34 820	18 attr.	−35 200
	interchain	0		10 attr.	
$(1A1R)^{er}(2A)^{ra}$	intrachain	0	−3293	18 attr.	−31 330
	interchain	5 repl.		5 attr., 5 repl.	
$(2A)^{er}(1A1R)^{ra}$	intrachain	9 repl.	−29 100	9 attr., 9 repl.	−33 110
	interchain	0		10 attr.	
$(2R)^{er}(2A)^{ra}$	intrachain	0	−2839	18 attr..	−8961
	interchain	10 repl.		10 repl.	
$(2A)^{er}(2R)^{ra}$	intrachain	18 repl.	−1750	18 repl.	−29 820
	interchain	0		10 attr.	
$(2R)^{er}(2R)^{ra}$	intrachain	18 repl.	−843	18 repl.	−3292
	interchain	5 repl.		10 repl.	

[a] Buffer conditions: pH 2.0, 25 mM phosphoric acid; pH 6.5, 10 mM phosphate, 1.0 mM EDTA.
[b] Nomenclature is as described in Table 1 and superscripts indicate whether the interaction is interchain (er) or intrachain (ra).
[c] The total number of potential intrachain (i, $i+3$ or i, $i+4$) and interchain (i, $i'+5$) interactions in the 36-residue two-stranded molecule.
[d] Ellipticity was measured at 5°C and 222 nm wavelength.
[e] 0 stands for no electrostatic interactions, attr. for attraction and repl. for repulsion.

4. Results

4.1. Circular dichroism spectroscopy

The far-UV CD spectra of the coiled-coil peptides at 5°C, pH 6.5 are shown in Fig. 4a. CD spectra of the same peptides but in the unfolded form, achieved either by high temperature (95°C) or by sequence rearrangement, are shown in Fig. 4b. Fig. 4c is the unfolding process of peptide $(2A)^{er}(2R)^{ra}$ as pH changes from 10 to 2. The spectra of folded peptides have two minima at 222 nm and 208 nm with a 222:208 ratio of about 1.03 in folded peptides, indicating the formation of coiled-coil structure [14,32]. The isodichroic point at 203 nm (Fig. 4c) indicates that each residue can exist in only two conformations, helical or non-helical [39,40].

Fig. 5a shows the pH dependency of ellipticity.

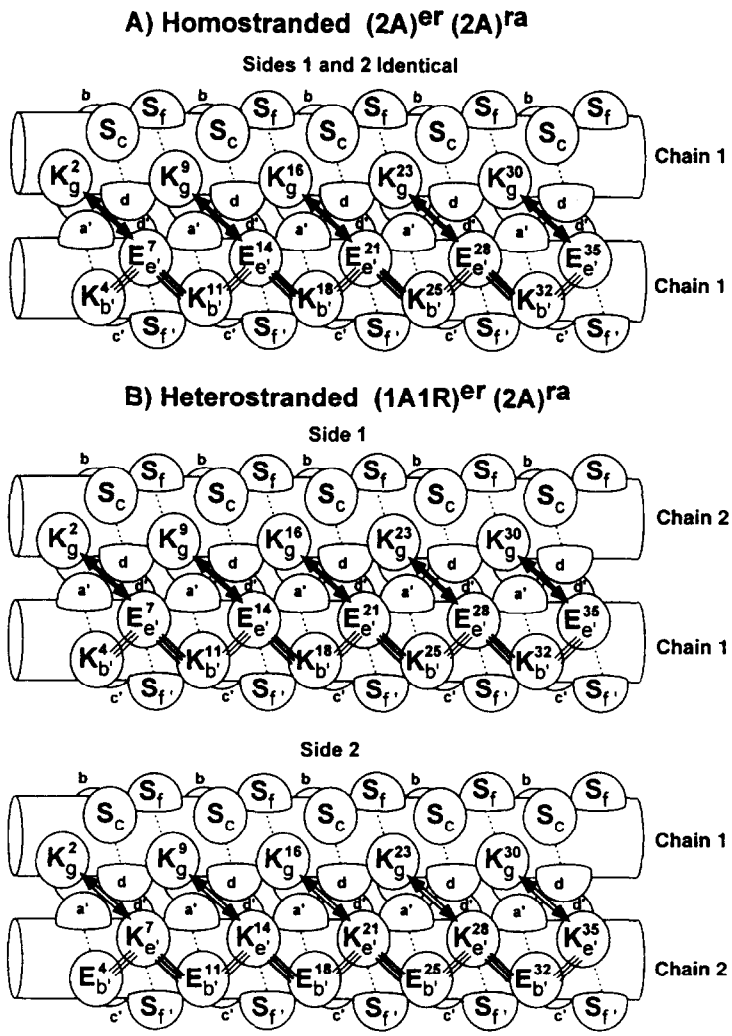

Fig. 3. Helical-rod diagrams of (A) a representative homostranded coiled-coil where the two sides are identical and (B) a heterostranded coiled-coil where the two sides are different. The solid arrows represent the $(i, i' + 5)$ interchain electrostatic attractions, the open arrows for $(i, i' + 5)$ interchain electrostatic repulsions, the bold bars for $(i, i + 4)$ intrachain electrostatic interactions and the thin bars for $(i, i + 3)$ intrachain electrostatic interactions. The chain numbers correspond to those in Table 1 and Fig. 2.

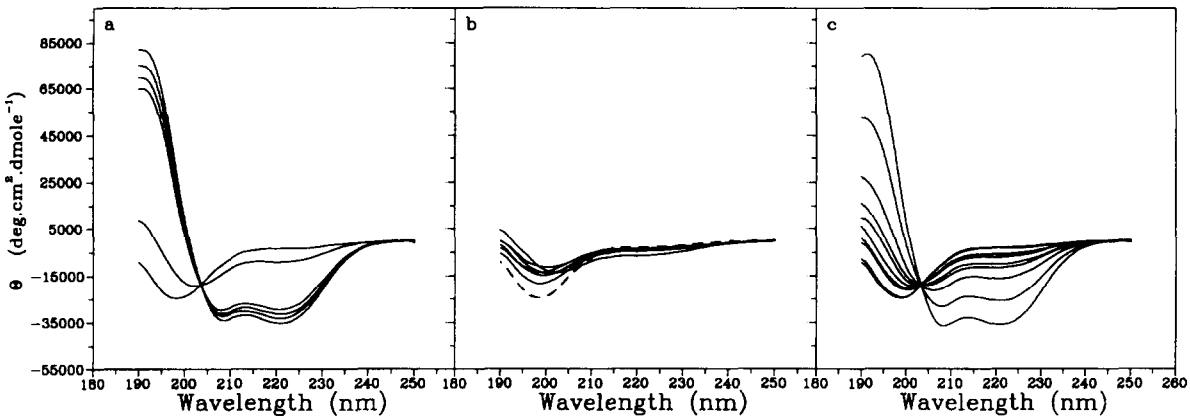

Fig. 4. CD spectra of folded and unfolded coiled-coils. (a) CD spectra of the peptides at 5°C, pH 6.5, in increasing order of ellipticity at 222 nm: $(2R)^{er}(2R)^{ra}$, $(2R)^{er}(2A)^{ra}$, $(2A)^{er}(2R)^{ra}$, $(1A1R)^{er}(2A)^{ra}$, $(2A)^{er}(1A1R)^{ra}$, $(2A)^{er}(2A)^{ra}$. (b) CD spectra of the peptides at 85°C, solid lines are: $(1A1R)^{er}(2A)^{ra}$, $(2A)^{er}(2R)^{ra}$, $(2A)^{er}(1A1R)^{ra}$ and $(2A)^{er}(2A)^{ra}$ at pH 6.5 and $(2A)^{er}(1A1R)^{ra}$ and $(2A)^{er}(2A)^{ra}$ at pH 2.0. Dashed lines are CD scans at 5°C for $(2R)^{er}(2A)^{ra}$ at pH 2.0 and $(2R)^{er}(2R)^{ra}$ at pH 6.5 (they almost superimpose each other). (c) CD spectra of peptide $(2R)^{er}(2A)^{ra}$ at pH 2.0, 3.0, 4.0, 5.0, 6.0, 7.0, 8.0, 9.0, 9.5, and 10.0 at 5°C, shown with increasing order of ellipticity. Buffers used: pH 2.0, phosphoric acid; 2.5–3.5, 10 mM glycine–HCl; 4.0–5.5, 10 mM sodium acetate, 1.0 mM EDTA; 6.0–7.5, 10 mM sodium phosphate, 1.0 mM EDTA; 8.0–10, 10 mM boric acid–NaOH, 1.0 mM EDTA.

The abrupt increase in ellipticity of peptides $(1A1R)^{er}(2A)^{ra}$ and $(2A)^{er}(2R)^{ra}$ at pH 4.0 was caused by the addition of EDTA. However, EDTA has no significant effect on ellipticity of any peptide between pH 6 and 7, where calorimetric measurements on fully charged coiled-coils take place. Fig. 5b shows the melting profiles of coiled-coils heated in low ionic strength solutions monitored by θ_{222}. Fig. 6 shows the effect of NaCl on the melting profiles of $(2A)^{er}(2A)^{ra}$ at pH 2.0 and 6.5.

4.2. Calorimetry

The CD results showed that, at low pH, only the peptide $(2A)^{er}(2A)^{ra}$ formed a stable coiled-coil, so calorimetric measurements were focused on this peptide. The heat capacity profiles of this peptide at different pH values are shown by Fig. 7a.

Another focus in the calorimetric measurements is pH 6.5, where both glutamate and lysine residues are expected to be charged and all the potential electrostatic attractions and repulsions are present. At this pH, four peptides, $(2A)^{er}(2A)^{ra}$, $(1A1R)^{er}(2A)^{ra}$, $(2A)^{er}(1A1R)^{ra}$ and $(2A)^{er}(2R)^{ra}$, form stable coiled-coils according to the CD spectra (Fig. 4a) and the results of calorimetric measurements of these peptides are presented in Fig. 7b. The inset in this figure shows the heat capacity of the unfolded peptides at pH 2.0 and 6.5. As can be seen, different peptides with the same composition have virtually

Table 3
Calorimetric data of unfolding coiled-coil peptides [a]

Peptide	pH	T_t (°C)	ΔH_{cal} [b]	ΔH_{vH} [b]	ΔH (70°C)	ΔS (70°C)	ΔG (70°C)
$(2A)^{er}(2A)^{ra}$	2.0	55.5	186	184	200	0.608	−8.6
	3.5	67.0	173	169	173	0.510	−4.0
	4.5	72.2	165	163	162	0.468	1.0
	6.5	86.3	166 [c]		144	0.400	7.1
$(2A)^{er}(1A1R)^{ra}$	6.5	78.2	156 [c]		144	0.410	3.6
$(2A)^{er}(2R)^{ra}$	6.5	70.5	145	144	144	0.420	0.2

[a] Enthalpies and free energies are in kJ mol^{-1}. Entropies are in kJ K^{-1} mol^{-1}.
[b] ΔH_{cal} and ΔH_{vH} are calorimetric and Van't Hoff enthalpies at T_t, respectively.
[c] Extrapolated values, see text for detail.

the same heat capacity for the unfolded state, which is in a very good correspondence with the calculated heat capacity for a fully extended peptide of the same composition.

Fig. 7 shows that the apparent heat capacities of all studied peptides drop at neutral pH (starting at pH 5.5) when the temperature of solution approaches 90°C. The drop becomes more severe in basic pH region (data not shown) and this is the reason why calorimetric measurements were not carried out in the basic pH region. The drop of the apparent heat capacity indicates the release of heat with increasing temperature caused by some irreversible processes. It cannot be caused by aggregation of unfolded peptides since we did not find a concentration dependence of this effect or visible aggregates in the solution after heating. Aggregation induced by hydrophobic interactions is not expected to have such a pH dependency. For the following reasons, this phenomenon is most likely due to chemical modification of disulfide bond. First, the observed irreversible release of heat by the studied peptides upon heating has the same pH dependence as the chemical modification of disulfide bond [30,31]. Second, the sample gave a strong smell of thiol group after heating up to 100°C at neutral pH. Finally, the irreversible release of heat upon heating disappeared when the cysteines in the polypeptides were replaced by valines (Fig. 8a). Unfortunately, without disulfide cross-linking, peptides $(1A1R)^{er}(2R)^{ra}$ and $(2A)^{er}(1A1R)^{ra}$ would form a heterogeneous mixture of three dimers. Thus this disulfide bond is vital for the quantitative study of the energetics of coiled-coils and cannot be eliminated.

The irreversible heat release at elevated tempera-

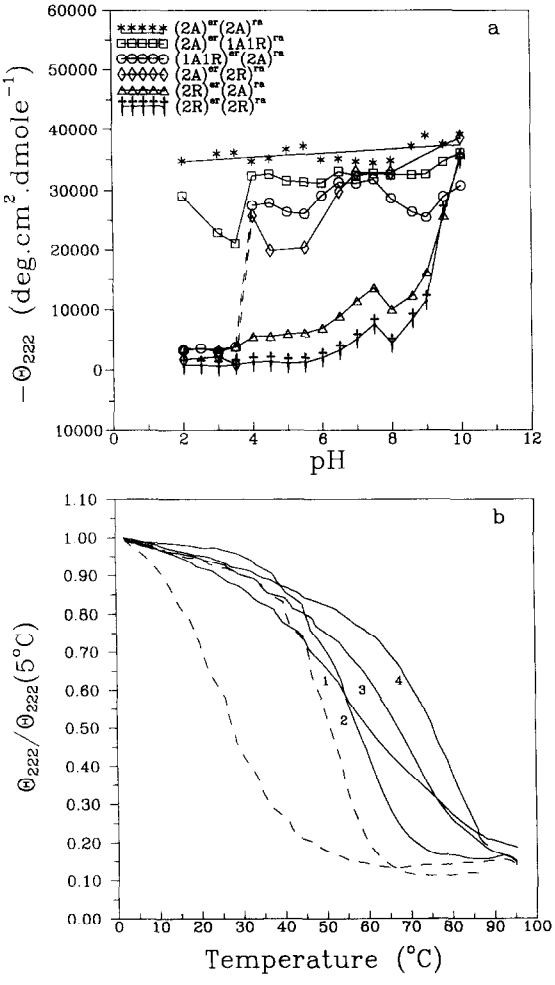

Fig. 5. Dependence of ellipticity of the peptides at 222 nm (Θ_{222}) on (a) pH and (b) temperature (normalized by the value at 5°C). In (b), solid lines represent the peptides at pH 6.5: 1 for $(1A1R)^{er}(2A)^{ra}$, 2 for $(2A)^{er}(2R)^{ra}$, 3 for $(2A)^{er}(1A1R)^{ra}$ and 4 for $(2A)^{er}(2A)^{ra}$. Dashed lines from left to right represent the peptides $(2A)^{er}(1A1R)^{ra}$ and $(2A)^{er}(2A)^{ra}$ at pH 2.0. The buffers used are the same as given in Fig. 4.

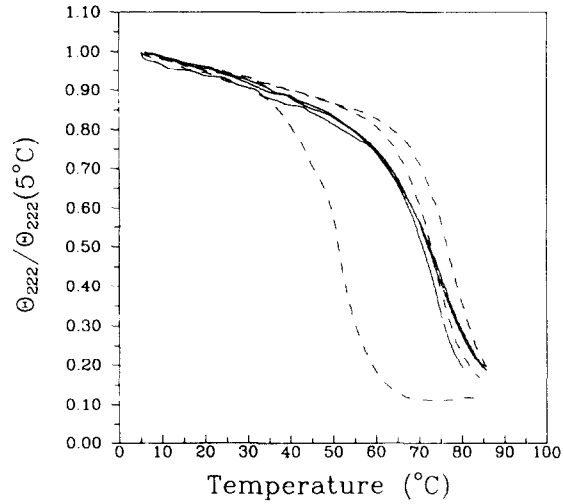

Fig. 6. Effect of sodium chloride on the thermal unfolding of $(2A)^{er}(2A)^{ra}$ at two pH values. Solid lines are at pH 6.5 in 10 mM sodium phosphate, 1.0 mM EDTA containing, from left to right 0 mM, 100 mM, 150 mM NaCl. Dashed lines are at pH 2.0 in dilute phosphoric acid containing, from left to right, 0 mM, 100 mM, 150 mM NaCl.

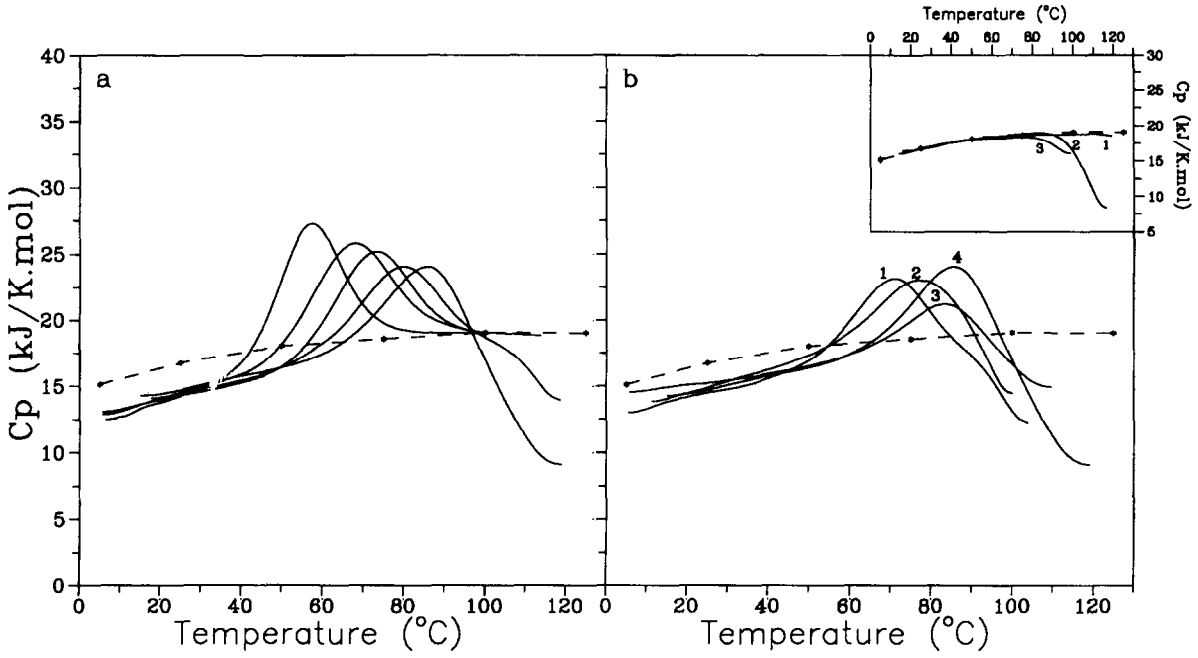

Fig. 7. Heat capacity of coiled-coils as function of temperature. (a) Peptide $(2A)^{er}(2A)^{ra}$ from left to right are at pH 2.0, 3.5, 4.5, 5.5 and 6.5. (b) Peptides $(2A)^{er}(2R)^{ra}$, $(2A)^{er}(1A1R)^{ra}$, $(1A1R)^{er}(2R)^{ra}$ and $(2A)^{er}(2A)^{ra}$ at pH 6.5, numbered 1, 2, 3 and 4, respectively. Inset: heat capacities of unfolded coiled-coils: 1, $(2R)^{er}(2A)^{ra}$ at pH 2.0; 2, $(2R)^{er}(2A)^{ra}$ at pH 6.5; 3, another reference peptide generated by residue shuffling but not included in the ensemble listed here. In all graphs, the dashed–starred line is the calculated heat capacity of the fully extended peptide according to its amino acid composition. The buffers used are the same as in Fig. 4.

ture is a serious obstacle for calorimetric measurements of the heat of unfolding of coiled-coils in conditions when they are stable and unfold at temperatures close to 85–90°C. However, in that case the total heat of unfolding can be determined from the first half of this process which takes place below 85°C [41]. Since we know the heat capacity increment upon unfolding of the peptides and know that unfolding is approximated by a two-state transition (as confirmed by results in the acidic pH region where there is no heat capacity drop after transition), we can evaluate with a good accuracy the complete heat capacity and enthalpy function of this process by its initial phase. This procedure is provided by the software developed for the calorimetry data processing at the Johns Hopkins Biocalorimetry Center. Fig. 8b shows an example of such analysis: the original heat capacity curve of $(2A)^{er}(2R)^{ra}$ at pH 6.5 and the simulated complete heat capacity function obtained from the first half of the observed heat absorption.

The unfolding enthalpies and entropies at the transition temperature are given in Table 3. For the purpose of comparison, Table 3 also lists all the thermodynamic quantities of stable coiled-coils extrapolated to 70°C, the temperature is selected to minimize the error of extrapolation.

5. Discussion

5.1. Is the unfolding process of cross-linked coiled-coils a two-state transition?

The answer is yes, in most cases. In this study, the coiled-coil peptide is unfolded by three means: rearrangement of sequence, pH and temperature. As peptides in the ensemble change stepwise from $(2A)^{er}(2A)^{ra}$ to $(2R)^{er}(2R)^{ra}$, the conformation at a given pH switches from a coiled-coil to random coil (Fig. 4a). Changing pH can also unfold a coiled-coil (Fig. 4c). The existence of an isodichroic point at 203 nm (Fig. 4a, c) suggests that in both processes

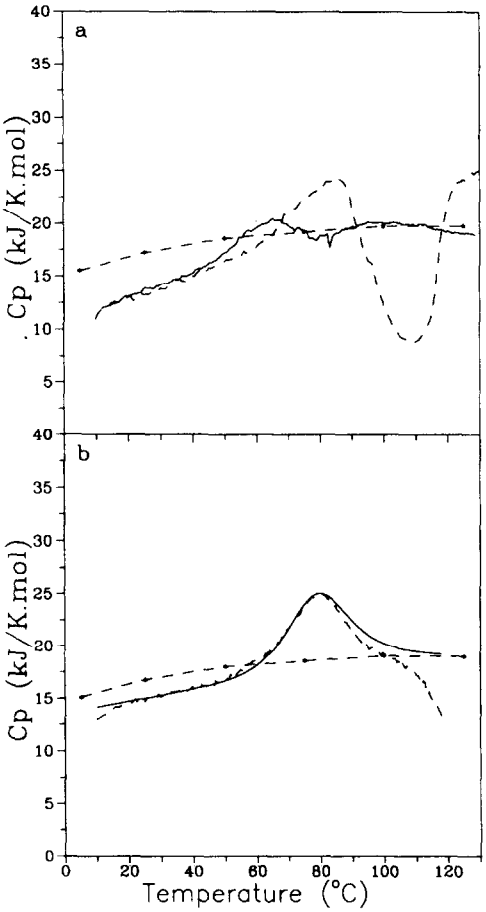

Fig. 8. (a) Effect of disulfide bond on the heat capacity drop of $(2A)^{er}(2A)^{ra}$ upon unfolding at neutral pH. Dashed line is the peptide with the disulfide bond. Solid line is the peptide without the disulfide bond (the two cysteines are replaced by valines). Buffer is 10 mM sodium phosphate, pH 7.0. 1 mM EDTA greatly alleviated the heat capacity anomaly at neutral pH when there is a disulfide bond, as evidenced by Fig. 7. (b) Simulation of the heat capacity of $(2A)^{er}(2R)^{ra}$ at pH 6.5 in 10 mM sodium phosphate, 1 mM EDTA. The dashed line is the actual heat capacity and the solid line is the simulated complete transition heat capacity profile. In both a and b, the dashed-starred line is the heat capacity of fully extended peptide calculated from the amino acid composition.

each residue can adopt only two possible conformations [39,40]. However, this does not necessarily mean that the unfolding of the whole molecule is a cooperative two-state transition. The cooperativity is shown by the thermal unfolding process.

The thermal unfolding of coiled-coils is monitored by both CD spectroscopy and calorimetry. The ellipticity profiles of most coiled-coils show a sharp sigmoidal transition as the temperature increases from 5 to 85°C, except for $(1A1R)^{er}(2A)^{ra}$ at pH 6.5 and $(2A)^{er}(1A1R)^{ra}$ at pH 2.0 (Fig. 5b). A sigmoidal transition again suggests a two-state process. However, the most definitive proof that the thermal unfolding of cross-linked coiled-coils is two-state comes from calorimetry. The Van 't Hoff enthalpy calculated based on a two-state transition is very close to the real, calorimetrically measured enthalpy of unfolding (Table 3). According to Thompson et al. [42], thermal unfolding of a non-cross-linked coiled-coil is also a two-state transition in the case of GCN4 leucine zipper.

However, it appears that unfolding of coiled-coils is not always a two-state transition. The temperature dependency of ellipticity at 222 nm indicates that the thermal unfolding of $(1A1R)^{er}(2A)^{ra}$ at pH 6.5 is much less cooperative process than that of the other peptides studied. $(2A)^{er}(1A1R)^{ra}$ at pH 2.0 gives a small tail phase (Fig. 5b) in melting. Calorimetrically, $(1A1R)^{er}(2A)^{ra}$ has a significantly higher pretransition heat capacity and much lower transition peak (Fig. 7b) compared to the other coiled-coils at pH 6.5. The thermal unfolding of $(2A)^{er}(1A1R)^{ra}$ at pH 2.0 gives a heat capacity profile that can be deconvoluted into two overlapping transitions, with the second one much smaller than the first one (data not shown), consistent with the CD results. These results suggest that the unfolding of certain coiled-coils could be more complex than a two-state transition under certain conditions. However, the cause of the observed deviation of their unfolding from a simple two-state transition is unclear. Further studies are needed to elucidate the origin of complex behavior of these peptides.

5.2. Are electrostatics important for coiled-coil stabilization?

The answer is yes, with subtleties. It appears that electrostatic attractions are not needed for the formation of coiled-coils. This follows from the experimental fact that a coiled-coil is formed at two extreme pH regions in which electrostatic attractions are absent. At low pH (2–3), glutamate is protonated

and does not form an ionic pair with lysine. In this region, $(2A)^{er}(2A)^{ra}$ has no electrostatic interactions but forms a stable coiled-coil (Fig. 5a). The ellipticity of $(2A)^{er}(2A)^{ra}$ is virtually independent of pH with an average of $-36\,120 \pm 1530$ deg cm^2 dmol^{-1}, which corresponds to about 100% helicity according to Zhou et al. [43]. On the other hand, as pH goes to 10, all peptides start to form stable coiled-coils, as indicated by the convergence of their ellipticities to that of $(2A)^{er}(2A)^{ra}$ (Fig. 5a). As the pH approaches 10, lysine residues deprotonate and lose their charges. As a result, all electrostatic attractions vanish in all peptides studied. Thus it appears that a coiled-coil is formed in the absence of significant electrostatic attractions. This is consistent with previous results [17,19,20] which showed that coiled-coils were formed when the *e* and *g* positions were all occupied by Gln which is not capable of forming interchain electrostatic interactions. Furthermore, a coiled-coil is not only formed in the absence of electrostatic interactions, but is also stable. For instance, at pH 2.0 $(2A)^{er}(2A)^{ra}$ has a T_m of 55.5°C with an unfolding enthalpy of about 23 J g^{-1}, comparable to the average of other multidomain coiled-coils and globular proteins [44]. These observations lead to the unambiguous conclusion that electrostatic attractions are not necessary in forming coiled-coils. This also explains the earlier observation that ion pairs are not required for leucine zipper activity [9]. The hydrophobic packing interaction at the helical interface and hydrogen bonding appear be the major force that drives the formation and stabilization of coiled-coils. However, our results show that electrostatic interactions also affect the stability of coiled-coils.

Of the two types of electrostatic interactions, namely repulsion and attraction, repulsion is much more straightforward. At pH 2.0, the total number of repulsions in the coiled-coils generated by residue shuffling varies from 0 to 23 (Table 2), with no attractions present and a constant number of charges. Therefore, the difference between the stabilities of these peptides could be caused only by the electrostatic repulsions. The results (Table 2 and Fig. 5a) show that coiled-coils have very little tolerance to electrostatic repulsions if there are no balancing attractions. One interchain repulsion in each heptad (a total of five for the coiled-coil) is enough to disrupt the structure entirely, as in the case of $(1A1R)^{er}(2A)^{ra}$ at pH 2.0. Intrachain repulsions are less disrupting in the sense that the coiled-coil structure is maintained in the presence of nine pairs of intrachain repulsion [$(2A)^{er}(1A1R)^{ra}$ at pH 2.0]. Only in the presence of 18 pairs of intrachain repulsion [$(2A)^{er}(2R)^{ra}$ at pH 2.0] is the coiled-coil structure completely unfolded (Fig. 5a). However, even though one intrachain repulsion in each heptad does not completely disrupt the coiled-coil structure, the peptide $(2A)^{er}(1A1R)^{ra}$ was only marginally stable at pH 2.0 and has lost its cooperativity. The very fact that repulsions are very destabilizing to coiled-coils hampered the attempt to measure its effect quantitatively by calorimetry because only one peptide, $(2A)^{er}(2A)^{ra}$, is stable at pH 2.0.

Our conclusion that electrostatic repulsions severely destabilize coiled-coils came as not much of a surprise since it agrees with the previous observation that electrostatic repulsions are mainly responsible for the preferential hetero-dimerization of Fos–Jun leucine zipper [8] and de novo coiled-coil models, where in all cases homodimer formation was prevented or destabilized by electrostatic repulsions [18–20,23]. It also agrees with the observation that electrostatic interactions, mostly repulsions, control the orientation of two-stranded coiled-coils [45].

The situation with electrostatic attractions is very different. It has long been noticed that muscle proteins like tropomyosin and paramyosin, which form long, multidomain coiled-coils, are more stable at low pH than at neutral pH [6,7]. This is surprising because these proteins have no electrostatic attractions at pH 2.0. Later, the same effect of greater stability at low pH was observed in short coiled-coils [13–17,23]. Lumb and Kim [24] recently observed that an ion pair in GCN4 leucine zipper is unfavorable, consistent with previous observations. However, our results show clearly the opposite trend, that the coiled-coils are more stable at neutral pH than at acidic pH (Figs. 5 and 6, and Table 3). Furthermore, elevating pH from 2 to 6.5 not only stabilizes coiled-coils, such as $(2A)^{er}(2A)^{ra}$ and $(2A)^{er}(1A1R)^{ra}$ (Fig. 5b), but it also refolds unfolded coiled-coils, such as $(1A1R)^{er}(2A)^{ra}$ and $(2A)^{er}(2R)^{ra}$ (Fig. 5a). These results clearly indicate that charged glutamate stabilizes a coiled-coil conformation more than protonated glutamate and that ion pairs contribute posi-

tively to the stability of this coiled-coil under our low ionic strength buffer conditions.

How do we reconcile our results with previous observations that coiled-coils are more stable at low pH? The answer comes from the difference in ionic strength. In all the previous studies, a significant amount of NaCl or KCl was present in the solution. Its concentration ranged from 0.1 M to 0.5 M [6,13–17,23,24]. On the other hand, the buffer solutions used in our experiments are only 10 mM in concentration and contain no NaCl. As Fig. 6 shows, in the presence of 0.1 M NaCl the $(2A)^{er}(2A)^{ra}$ coiled-coil is indeed slightly more stable at pH 2.0 than at 6.5 and 0.15 M NaCl makes the peptide significantly more stable at pH 2.0 than at 6.5. Also from Fig. 6, it can be seen that NaCl has more pronounced effect at pH 2.0 while it has very little effect at pH 6.5, which agrees with the observation that the T_t of a leucine zipper is relatively independent of ionic strength at pH 7 [23]. Judging from these results, the increased stability of coiled-coils at low pH might be caused by the presence of salt. The effect of NaCl could result from shielding and binding. It is well known that electrostatic interactions could be significantly shielded by salt. This shielding effect of NaCl would reduce the strength of attractions which are present only at neutral pH. On the other hand, non-specific anion binding should be enhanced at pH 2.0 due to the increase in net positive charges carried by the peptide. Thus, the effect of NaCl could also result from binding of anions to the positively charged lysine side chains, which are near the hydrophobic core, and this would enhance the relative stability of coiled-coils at acidic pH versus neutral pH. This resembles the so-called counterion condensation encountered in double-stranded-helical DNA [46,47]. One cannot exclude, however, that the high concentration of electrolyte might affect properties of water and consequently, the hydrophobic effect [16,20]. In order to avoid the complex effect of salt, we chose low ionic strength instead of physiological buffer conditions to reveal the full strength of electrostatic interactions. This is especially important in the case of coiled-coils because all the interactions are on the surface.

Based on our experimental results, we conclude that coiled-coils can be significantly stabilized by electrostatic attractions in the absence of salt. A more detailed study on the pH and salt effect on the stability of coiled-coil, employing both thermal and chemical denaturation, is presented elsewhere [48].

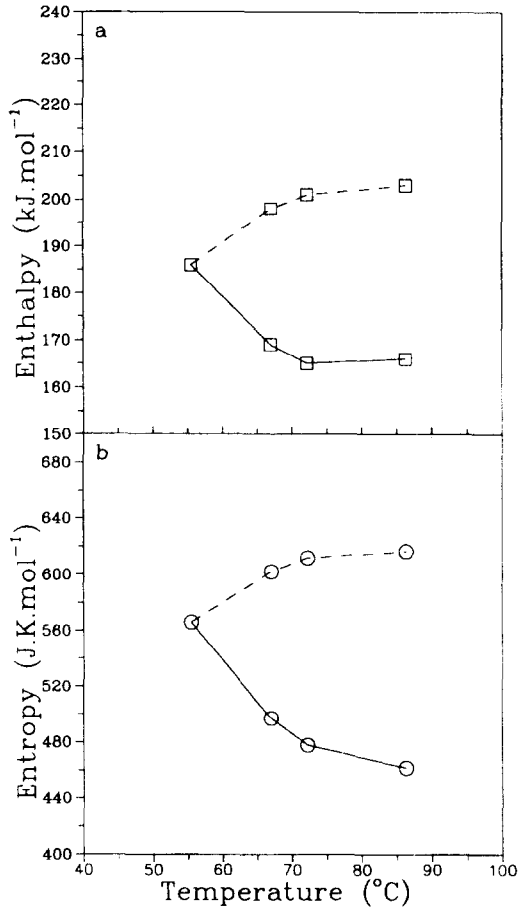

Fig. 9. Temperature dependencies of (a) enthalpy and (b) entropy of unfolding of $(2A)^{er}(2A)^{ra}$ coiled-coil. Solid lines show experimental values obtained by calorimetric measurements of coiled-coil unfolding in solutions at pH 2.0, 3.5, 4.5 and 6.5 (left to right, respectively); dashed lines show the enthalpy and entropy of unfolding of coiled-coil, calculated by Eqs. 1 and 2, assuming that all glutamates are protonated.

5.3. With positive ΔC_p, why does unfolding enthalpy decrease as transition temperature increases?

Although the fact that ion pairs stabilize a coiled-coil is expected, the pH-induced increase in the electrostatic interactions results in a quite unexpected phenomenon: with increase in stability, i.e. transition temperature T_t, upon changing pH from 2 to 6.5, the

enthalpy of unfolding $(2A)^{er}(2A)^{ra}$ decreases (Figs. 7 and 9a and Table 3), in sharp contrast to what normally happens in globular proteins [41]. Similarly, ΔS also decreases with pH (Fig. 9b). This decrease in the unfolding enthalpy and entropy with an increase in pH and transition temperature cannot be associated with the irreversible heat release caused by hydrolysis of cystines, which only happens at neutral pH and high temperature. But it is most likely caused by deprotonation of glutamate as the pH goes from 2 to 6.5.

In general, ΔH should be a function of both temperature and pH. However, if unfolding enthalpy and heat capacity increment would be pH independent, as one can expect for the pH 2.0 solution in which all glutamates are protonated and no significant deprotonation is expected with temperature increase, then the enthalpy would appear as an increasing function of temperature with a slope equal to the heat capacity increment:

$$\Delta H(T, \mathrm{pH}_1 = 2)^{cal} = \Delta H(T_t, \mathrm{pH}_1 = 2) + \int_{T_t}^{T} \left(\frac{\partial \Delta H}{\partial T} \right)_{\mathrm{pH}} \mathrm{d}T = \Delta H(T_t, \mathrm{pH}_1 = 2) + \int_{T_t}^{T} \Delta C_p \mathrm{d}T \quad (1)$$

This function is plotted in Fig. 9a, together with $\Delta H(T, \mathrm{pH})^{exp}$, the experimental unfolding enthalpy determined calorimetrically at various pH values. It is interesting to see that the calculated and the experimental enthalpy values show opposite trends when plotted against transition temperature.

A similar situation holds for the entropy of unfolding of coiled-coils. In the absence of pH-induced changes in the state of ionized groups, the entropy of coiled-coil unfolding should be an increasing function of temperature:

$$\Delta S(T, \mathrm{pH}_1 = 2)^{cal} = \Delta S(T_t, \mathrm{pH}_1 = 2) + \int_{T_t}^{T} \left(\frac{\partial \Delta S}{\partial T} \right)_{\mathrm{pH}} \mathrm{d}T = \frac{\Delta H(T_t, \mathrm{pH}_1 = 2)}{T_t} + \int_{T_t}^{T} \Delta C_p \mathrm{d} \ln T \quad (2)$$

Instead, the entropy of unfolding measured calorimetrically at various pH decreases with the increase of transition temperature (Fig. 9b).

Deviation of the calculated functions from the experimentally determined unfolding enthalpies and entropies corresponds to the pH-induced effect caused by increase in the number of deprotonated glutamates:

$$\delta\Delta H(T, \mathrm{pH})^{ion} = \Delta H(T, \mathrm{pH})^{exp} - \Delta H(T, \mathrm{pH}_1 = 2)^{calc} \quad (3)$$

$$\delta\Delta S(T, \mathrm{pH})^{ion} = \Delta S(T, \mathrm{pH})^{exp} - \Delta S(T, \mathrm{pH}_1 = 2)^{calc} \quad (4)$$

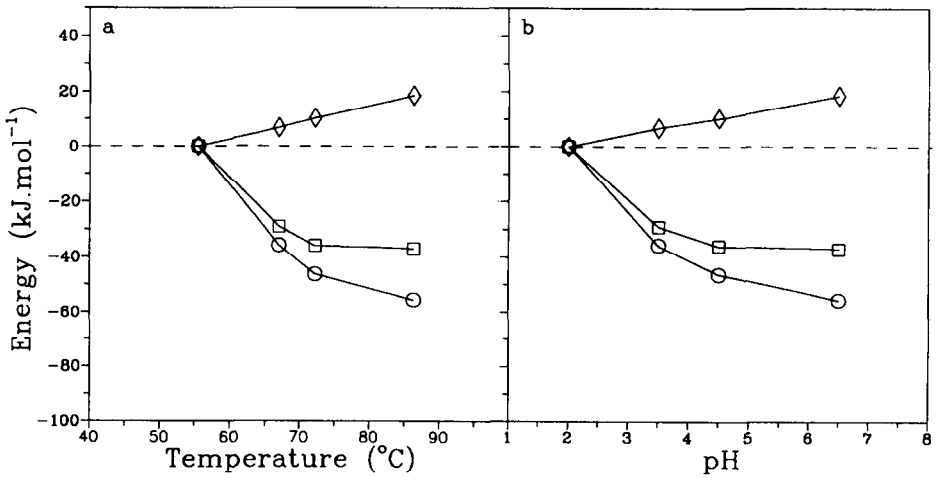

Fig. 10. The temperature dependence (a) and the pH dependence (b) of the contribution of electrostatic interactions to the stabilization of the $(2A)^{er}(2A)^{ra}$ coiled-coil calculated by Eqs. 3, 4 and 6. Square represents $\delta\Delta H(T, \mathrm{pH})^{ion}$, circle represents $T\delta\Delta S(T, \mathrm{pH})^{ion}$, and diamond represents $\delta\Delta G(T, \mathrm{pH})^{ion}$.

It appears that the disruption of the contact between the negatively charged glutamate and positively charged lysine and the exposure of these charged groups to water is associated with negative enthalpy and entropy effects (Fig. 10). Their negative values result certainly not from disruption of electrostatic interaction between the opposite charged groups but from the hydration of these groups. In $(2A)^{er}(2A)^{ra}$, each glutamate is surrounded by three lysines (Fig. 3). Therefore, their side chains would be at least partly shielded from water by each other. In the unfolded form, there is no stable ion pairs and the side chains of lysines and glutamate would be fully exposed to water. This will result in change of their hydration status upon unfolding. It is known that the enthalpy and entropy of hydration of charged groups are negative and large in magnitude [49,50]. In these coiled-coils the pH dependence of this effect is mainly due to glutamate because the lysine side chains do not change their charge upon changing pH from 2.0 to 6.5. In globular proteins the similar effect of pH-induced decrease of unfolding enthalpy was not observed experimentally because there are not many buried or partly buried ion pairs.

5.4. Contribution of electrostatic interactions to the stabilization of coiled-coils

Although the enthalpy and entropy of unfolding of these coiled-coils decreased with rising the pH from 2.0 to 6.5, the Gibbs energy,

$$\Delta G(T,\mathrm{pH}) = \Delta H(T,\mathrm{pH}) - T\Delta S(T,\mathrm{pH}) \qquad (5)$$

increases with pH, as evidenced by the increase in T_t with pH. Correspondingly we found that the Gibbs energy associated with deprotonation of glutamate, defined by

$$\delta\Delta G(T,\mathrm{pH})^{ion} = \delta\Delta H(T,\mathrm{pH})^{ion} - T\delta\Delta S(T,\mathrm{pH})^{ion} \qquad (6)$$

is positive (Fig. 10a). It appears that deprotonation of glutamate resulting from increasing pH to 6.5 led to a smaller decrease in enthalpy than in the entropy of unfolding. This is understandable because unfolding of a coiled-coil is associated not only with hydration of charges but also with disruption of interaction between these charges. This requires some energy which is positive if the groups paired in the coiled-coil are charged oppositely. If, according to Lumry et al. [51], the enthalpy and entropy of hydration of these groups are compensating each other, then one could conclude that the observed $\delta\Delta G^{ion}$ results from the electrostatic interactions in the coiled-coil. In the $(2A)^{er}(2A)^{ra}$ coiled-coil at pH 6.5, when all glutamates are fully charged, this electrostatic effect amounts to 18.6 kJ mol^{-1} in terms of Gibbs energy. Neglecting the possible temperature dependence of $\Delta\Delta G^{ion}$ in the rather short temperature range 55–85°C, we can present the stabilizing effect of electrostatic interactions of the coiled-coil conformation at a medium temperature of 70°C as a function of pH (Fig. 10b).

The differences in electrostatic interactions between $(2A)^{er}(2A)^{ra}$ and $(2A)^{er}(1A1R)^{ra}$ and between $(2A)^{er}(1A1R)^{ra}$ are 3.5 kJ mol^{-1} and 3.4 kJ mol^{-1}, respectively, at 70°C. The folded forms of all coiled-coils in the ensemble have ten pairs of $(i, i+3)$ and eight pairs of $(i, i+4)$ intrachain interactions. In $(2A)^{er}(2A)^{ra}$, all are attractions. In $(2A)^{er}(1A1R)^{ra}$, half are attractions, half are repulsions. In $(2A)^{er}(2R)^{ra}$, all are repulsions. $(2A)^{er}(2A)^{ra}$, $(2A)^{er}(1A1R)^{ra}$ and $(2A)^{er}(2R)^{ra}$ have no difference in any other aspect (Fig. 2). Therefore, the 3.5 kJ mol^{-1} free energy difference is caused by these attractions versus repulsions. Assuming that attraction is of about the same magnitude as repulsion, the average strength of $(i, i+3)$ and $(i, i+4)$ intrachain electrostatic interaction appears to be about 0.2 kJ mol^{-1}. It must be emphasized that this results pertains only to low ionic strength buffer, where the salt effect on electrostatic interactions are not significant.

Acknowledgements

We thank Mr. P. Semchuk for the peptide synthesis and mass spectrometry and Ms. T. Keown for amino acid analyses. We also thank Dr. G. Privalov for doing the heat capacity simulation for us, as well as Dr. J.H. Carra and W.D. Kohn for reading the manuscript and giving valuable suggestions. This research is supported by the NIH grant GM48036-01 and NSF grant MCB 9118687, USA and the Protein Engineering Network of Centres of Excellence, Canada.

References

[1] C.B. Anfinsen, Science, 181 (1973) 223–230.
[2] G.I. Makhatadze and P.L. Privalov, Adv. Protein Chem., 47 (1995) 307–425.
[3] F.H.C. Crick, Acta Crystallogr., 6 (1953) 689–697.
[4] E.K. O'Shea, J.D. Klemm, P.S. Kim and T. Alber, Science, 254 (1991) 539–544.
[5] R.S. Hodges, Curr. Biol., 2 (1992) 122–124.
[6] S. Lowey, J. Biol. Chem., 240 (1965) 2421–2427.
[7] M. Noelken and A.M. Holtzer, in J. Gergely, (Ed.), Biochemistry of Muscle Contraction, Little, Brown and Co., Boston, 1964, pp. 374–378.
[8] E.K. O'Shea, R. Rutkowski and P.S. Kim, Cell, 68 (1992) 699–708.
[9] J.C. Hu, N.E. Newell, B. Tidor and R.T. Sauer, Protein Sci., 2 (1993) 1072–1084.
[10] W.F. Harrington, Proc. Natl. Acad. Sci. USA, 68 (1971) 685–689.
[11] W.F. Harrington, Proc. Natl. Acad. Sci. USA, 76 (1979) 5066–5070.
[12] R.S. Hodges, A.K. Saund, P.C.S. Chong, S.A. St.-Pierre and R.E. Reid, J. Biol. Chem., 256 (1981) 1214–1224.
[13] S.Y.M. Lau, A.K. Taneja and R.S. Hodges, J. Biol. Chem., 259 (1984) 13253–13261.
[14] R.S. Hodges, P.D. Semchuk, A.K. Taneja, C.M. Kay, J.M.R. Parker and C.T. Mant, Pept. Res., 1 (1988) 19–30.
[15] N.E. Zhou, B.Y. Zhou, C.M. Kay and R.S. Hodges, Biopolymers, 32 (1992) 419–426.
[16] R.S. Hodges, B.Y. Zhu, N.E. Zhou and C.T. Mant, J. Chromatogr. A, 676 (1994) 3–15.
[17] N.E. Zhou, C.M. Kay and R.S. Hodges, Protein Eng., 7 (1994) 1365–1372.
[18] N.E. Zhou, C.M. Kay and R.S. Hodges, J. Mol. Biol., 237 (1994) 500–512.
[19] W.D. Kohn, C.M. Kay and R.S. Hodges, Protein Sci., 4 (1995) 237–250.
[20] W.D. Kohn, O.D. Monera, C.M. Kay and R.S. Hodges, J. Biol. Chem., 270 (1995) 25495–25506.
[21] R.S. Hodges, J. Sodek, L.B. Smillie and L. Jurasek, Cold Spring Harbor Symp. Quant. Biol., 37 (1972) 299–310.
[22] A.D. McLachlan and M. Stewart, J. Mol. Biol., 98 (1975) 293–304.
[23] E.K. O'Shea, K.J. Lumb and P.S. Kim, Curr. Biol., 3 (1993) 658–667.
[24] K.J. Lumb and P.S. Kim, Science, 268 (1995) 436–439.
[25] J. Wojcik, K.-H. Altmann and H.A. Scheraga, Biopolymers, 30 (1990) 121–134.
[26] P.J. Gans, P.C. Lyu, M.C. Manning, R.W. Woody and N.R. Kallenbach, Biopolymers, 31 (1991) 1605–1614.
[27] K.T. O'Neil anf W.F. Degrado, Science, 250 (1990) 646–651.
[28] A. Chakrabartty, T. Kortemme and R.L. Baldwin, Protein Sci., 3 (1994) 843–852.
[29] N.E. Zhou, O.D. Monera, C.M. Kay and R.S. Hodges, Protein Pept. Lett., 1 (1994) 114–119.
[30] T.J. Ahern and A.M. Klibanov, Methods Biochem. Anal., 33 (1988) 91–127.
[31] S. Clarke, R.C. Stephenson and J.D. Lowenson, in T.J. Ahern and M.C. Manning (Eds.), Stability of Protein Pharmaceuticals, Part A: Chemical and Physical Pathways of Protein Degredation, Plenum Press, New York, 1992, pp. 1–29.
[32] R.S. Hodges, N.E. Zhou, C.M. Kay and P.D. Semchuk, Pept. Res., 3 (1990) 123–137.
[33] O.D. Monera, N.E. Zhou, C.M. Kay and R.S. Hodges, J. Biol. Chem., 268 (1993) 19218–19227.
[34] S.C. Gill and P.H. von Hippel, Anal. Biochem., 182 (1989) 319–326.
[35] A.F. Winder and W.L.C. Gent, Biopolymers, 18 (1971) 1243.
[36] P.L. Privalov and S.A. Potekhin, Methods Enzymol., 131 (1986) 4–51.
[37] P.L. Privalov and G.I. Makhatadze, J. Mol. Biol., 213 (1990) 385–391.
[38] G.I. Makhatadze, V.N. Medvedkin and P.L. Privalov, Biopolymers, 30 (1991) 1001–1010.
[39] S. Padmanabhan, S. Marqusee, T. Ridgeway, T.M. Laue and R.L. Baldwin, Nature, 344 (1994) 268–270.
[40] M. Engel, R.W. Williams and B.W. Erickson, Biochemistry, 30 (1991) 3161–3169.
[41] P.L. Privalov and N.N. Khechinashvili, J. Mol. Biol., 86 (1974) 665–684.
[42] K.S. Thompson, C.R. Vinson and E. Freire, Biochemistry, 32 (1993) 5491–5496.
[43] H.X. Zhou, P. Lyu, D.E. Wemmer and N.R. Kallenbach, Proteins Struct. Funct. Genet., 18 (1994) 1–7.
[44] P.L. Privalov, Adv. Protein Chem., 35 (1982) 1–104.
[45] O.D. Monera, C.M. Kay and R.S. Hodges, Biochemistry, 33 (1994) 3862–3871.
[46] F. Oosawa, Biopolymers, 6 (1968) 145–158.
[47] G.S. Manning, Biopolymers, 11 (1972) 937–949.
[48] Y. Yu, O.D. Monera, R.S. Hodges and P.L. Privalov, J. Mol. Biol., 255 (1996) 367–372.
[49] G.I. Makhatadze and P.L. Privalov, J. Mol. Biol., 232 (1993) 639–659.
[50] P.L. Privalov and G.I. Makhatadze, J. Mol. Biol., 232 (1993) 660–679.
[51] R. Lumry, E. Battistel and C. Jolicoeur, Faraday Discuss. Chem. Soc., 17 (1982) 93–108.